Dynamical characteristics of geomorphologic evolution of the basins covered by Pisha-sandstone in the eastern wing of the Ordos Plateau, China

GU Zhen-kui[1,2] http://orcid.org/0000-0002-5023-7431; e-mail: bygzk853@126.com

SHI Chang-xing[1*] http://orcid.org/0000-0002-5324-2981; e-mail: shicx@igsnrr.ac.cn

** Corresponding author*

1 Key Laboratory of Water Cycle and Related Land Surface Processes, Institute of Geographic Sciences and Natural Resources Research, Chinese Academy of Sciences, Beijing 100101, China

2 University of Chinese Academy of Sciences, Beijing 100049, China

Citation: Gu ZK, Shi CX (2018) Dynamical characteristics of geomorphologic evolution of the basins covered by Pisha-sandstone in the eastern wing of the Ordos Plateau, China. Journal of Mountain Science 15(5). https://doi.org/10.1007/s11629-018-4859-8

Abstract: There are several basins with high sediment yield in the Pisha-sandstone covering area of the east wing of the Ordos Plateau. Due to the lack of targeted research on the dynamical characteristics of geomorphic evolution that plays an important role in the sand production, this paper analyzed the tectonic activity intensity and erosion characteristics of the area. The results show that the intensity of tectonic activities in the area is generally moderate-weak and shows an unconspicuous increase from north to south. Tectonic activity is manifested mainly in the form of uplift. The uplift rate in the lower reaches of each basin is greater than the erosion rate, which is prominent in the Kuyehe and the Tuweihe rivers. During the uplift of the regional topography, the most serious parts under erosion are generally concentrated in the upstream and midstream of basins. All longitudinal profiles of the basins have a shape close to an exponential function, which indicates that they are in the early stage of erosion evolution. The mechanisms of geomorphologic evolution of these basins have a great similarity. The conservative estimate of historical average erosion rate was less than 182–520 t/(km²·yr), much less than that of the modern times. The average stream power values are typically distributed between 4 and 102 W/m, with the larger being in the Kuyehe and the Tuweihe rivers and the smallest being in the Qinshuihe River. The maximum stream power value appears in the downstream reach, which should be the main reason for the particles being directly injected into the Yellow River. From the perspective of geomorphological evolution, the current soil and water conservation measures can hardly cure the erosion of these basins in the long run.

Keywords: Dynamic characteristics; Geomorphologic evolution; Ordos Plateau; Tectonic activity; Stream power; Geomorphological parameter

Received: 21 January 2018
Revised: 04 April 2018
Accepted: 14 April 2018

Introduction

The Ordos block is surrounded by graben basins, playing an important role in North China Cenozoic and modern tectonic activities (Deng et al. 1999). The internal tectonic activities of the block are fairly consistent, and the stratum structure is simple, reserving a large number of fluvial-lacustrine sedimentary rocks formed in the

Mesozoic (Ma 2007; Shi 2008). Since the Cenozoic, the block has been uplifted by the influence of the Qinghai-Tibet Plateau uplift and the vertical force caused by upwelling of material in the deep Earth interior flow (Deng et al. 1999). Probably, it completed the transition from basins to a plateau in the late Miocene-Pliocene period (Yue et al. 2007). During the uplifting of the block, the surface was constantly being eroded, and as the erosion being strengthened, a series of NW-SE oriented rivers developed in the eastern wing of the Ordos Plateau. The basement rocks in the basins where rivers are located are widely exposed, especially in the basins covered by Pisha-sandstone in the northern part. Owing to the particles in the sandstone are coarse and poorly cemented, the sediment yield in these basins is large and particles are directly transported to the Yellow River, which has an important impact on the formation of the sediment characteristics of the Yellow River. In recent years, a series of soil and water conservation measures implemented in the region have achieved remarkable results in reducing sediment load (Zhang et al. 2004; Ran et al. 2008; Liu and Liu 2010; Zuo et al. 2016). However, the evolution of the landscape is a long-term historical process. The implementation of soil and water conservation measures needs to take into account the dynamical characteristics of the landscape evolution. Over the past years, many scholars have done a great deal of research on the geomorphic evolution of the eastern edge of Ordos, such as the uplift rate of the block, the mode of movement, the relationship between blocks and the topography of the peripheral basins and others (Cheng et al. 2002; Pan et al. 2011; Gao et al. 2016a; Hu et al. 2016). Yet, the spatial scale of the issues discussed by these previous studies is large and more emphasis is placed on the exploration of tectonic activities of the whole Ordos block or the Jin-Shan Gorge, neglecting the comprehensive analysis of tectonic and erosive activities in a medium-scale space. This paper gives a preliminary analysis to this problem by investigating the dynamic characteristics of the geomorphologic evolution in the region from the aspects of intensity of regional tectonic activity, spatial differences of erosion features, dynamic characteristics of rivers and the evolution characteristics of the longitudinal profiles. The results will be of benefit to understanding the characteristics of sediment transport in the sediment sources of the Yellow River and are of great significance to further explain the internal and external environments of the area.

1 Study Area

The study area is located in the eastern Ordos Plateau and the northern Loess Plateau, including the basins of Huangfuchuan (HPC), Qinshuihe (QSH), Gushanchuan (GSC), Kuyehe (KYH) and Tuweihe (TWH) rivers from north to south, all of which are the tributaries of the Yellow River with a total area of about 2.0×10^4 km^2 and an elevation range of 717–1587 m (Figure 1). The surface of the basins is covered with thin Quaternary loess. The gully area exposes the fluvial-lacustrine sedimentary rocks formed in Mesozoic period (Ma 2007). The sedimentary rocks are predominantly purple, gray-green, or variegated sandstone, mudstone and conglomerate. Due to their loose structure, the rocks are susceptible to erosion, habitually collectively referred to as Pisha-sandstone. The whole area was uplifted in the Cenozoic and has likewise undergone several episodes of tectonic uplift activities since the Quaternary. The thick sedimentary rocks in the area are well-preserved with few active faults (Shi

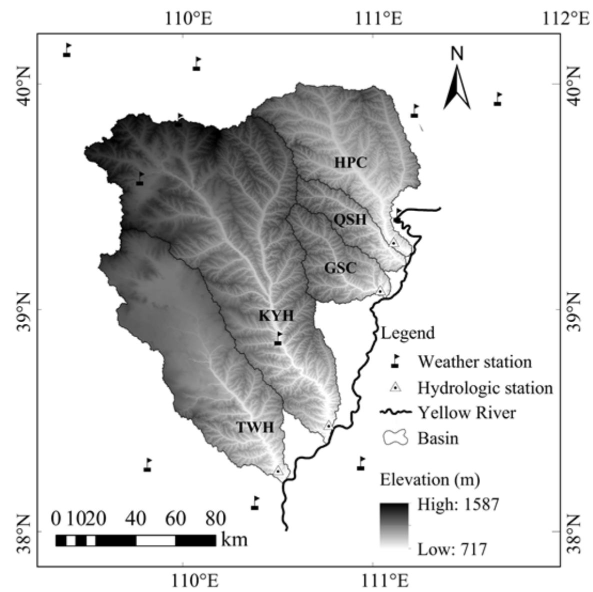

Figure 1 Study area. The five basins of the east wing of Ordos Plateau: Huangfuchuan (HPC), Qinshuihe (QSH), Gushanchuan (GSC), Kuyehe (KYH) and Tuweihe (TWH).

2008). The types of landscape can be sub-divided into sandy and hilly areas. The study area has a monsoon climate in the mainland, and the runoff is mainly recharged by precipitation.

2 Materials and Methods

2.1 Tectonic activity intensity

2.1.1 Quantitative indicators of landscape

The evolution of landscape of an area can record the information of tectonic activities occurred in the area. Using the quantitative indicators of landscape, the characteristics of neotectonic movement in the area can be recognized. Commonly used geomorphological indicators for analyzing tectonic activities include Hypsometric integral (*HI*), Asymmetry factor (*AF*), Stream length gradient index (*SL*), and Basin shape index (*Bs*). On a certain spatial scale, *HI* can be used to reflect the strength of the tectonic uplift activity and is generally divided into three levels, i.e., ≥0.7, 0.5-0.7, <0.5, respectively for the strong, moderate, and weak tectonic uplift. *AF* is used to evaluate tectonic tilt, and it is also divided into three grades. A value of $|AF\text{-}50|\geq 15$, 7-15, and <7 indicates that the tectonic activity is strong, moderate, and weak, respectively. *SL* is very sensitive to the change of slope in a longitudinal profile and can be used to reflect the strength of tectonic activity in areas with similar lithology characteristics (Mahmood and Gloaguen 2012). The *SL* rises when the river flows in an ascending zone and slightly lowers in a strike-slip zone. Three ranges of *SL* values are associated with three levels of tectonic activities, that is, $SL>500$ for the strong, $300\leq SL\leq 500$ for the moderate, and $SL\leq 300$ for the weak tectonic activities. In order to compare the steepness of a longitudinal profile at a generally uniform spatial scale, the index *SL* is usually normalized as SL/K (Ji et al. 2011). *Bs* is used to describe the horizontal projection shape of basins. It is also divided into three levels, that is, $Bs>3$ for the strong, $2\leq Bs<3$ for the moderate, and $Bs<2$ for the weak tectonic activities. Each of these indicators represents an aspect of tectonic activities, and three ranges of each indicator are assign a value from 1, 2 to 3 (Pike and Wilson 1971; Hack 1973; Ji et al. 2011; Mahmood and Gloaguen 2012; Gao et al. 2013; Ramírez-Herrera 2015; Gao et al. 2016b; Owono et al. 2016).

2.1.2 A composite index of tectonic activity intensity

Nowadays, it is a common practice to use the average grade value of geomorphological indicators for ranking the intensity of tectonic activities, that is,

$$IRAT = \frac{S_{HI} + S_{AF} + S_{SL} + S_{Bs}}{4} \quad (1)$$

where *S* is the activity intensity level of each geomorphological indicator, such as 1, 2 and 3. The *IRAT* (Index of relative active tectonics) value is generally divided into four levels from 1 to 4, with $1.0\leq IRAT<1.5$ for the maximum, $1.5\leq IRAT<2.0$ for the strong, $2.0\leq IRAT<2.5$ for the medium, and $2.5\leq IRAT<3$ for the weak tectonic activities (Gao et al. 2016b; Gao et al. 2013; Hamdouni et al. 2008).

2.2 Erosion characteristics analysis

2.2.1 Spatial differences of erosion characteristics

Spatial differences in erosion characteristics represent the different erosion history of basins, which are closely related to tectonic uplift and the intensity of hydraulic erosion. These features can be analyzed by the area-elevation curves and the estimation of the total erosion during the period of landform evolution. Among them, the area-elevation curve can reflect the intensity of the erosion more simply. In order to show the spatial differences of erosion history more clearly, the original terrain trend was fitted by the interpolation surface. As the higher elevation points along the ridges are often the residual surface of the original landscapes that were not eroded or were preserved under weak erosion, the total erosion of a basin can be estimated by calculating the elevation difference between this surface and the present surface based on the DEM data of the basin. The elevation of the highest point in a circular window of 20 km in diameter is extracted from the DEM data to build the original surface.

2.2.2 Average erosion rates

The average erosion rate can be calculated from the amount and time of erosion. Since the tectonic uplift is the most basic condition for erosion, the transition time of a surface from a plain to a plateau can be used as the starting time of erosion. Yue et al. (2007) argue that the Ordos Plateau was uplifted from a basin to a plateau probably during the late Miocene-Pliocene. Cheng et al. (2002) suggest that the plateau has experienced several uplifts since 1.41 Ma BP, with an initial uplift rate of 0.03–0.23 mm/yr and a recent uplift rate of 2.33 mm/yr. Similarly, a study on the Jin-Shan Canyon by Hu et al. (2016) shows that the tectonic uplift of the plateau has been obvious since the 1.2 Ma BP. Since the elevation of the plateau was not large at the initial stage of the uplift, the erosion activity would be greatly restricted. The period of active erosion should be after the surface reaches a certain height, so the 1.41 Ma BP is taken as the erosion initiation time used to calculate the historical average erosion rate. Since the basin area increases gradually during the evolution of a basin, the basin area for calculating sediment yield modulus is assumed to be half of the present basin area.

2.3 Dynamic characteristics of the longitudinal profile

2.3.1 Characteristics of functions fitting longitudinal profiles

The longitudinal profile of the main stream of a basin changes in its shape that can be fitted by a certain function in the order of "linear-exponential-logarithm-power" with the evolution of landform erosion (Rădoane et al. 2003). In the initial period of erosion, the longitudinal profile is close to a straight line. With the erosion and downstream deposition, the concavity of longitudinal profile will increase and the profile will evolve into an exponential morphology, then into a relatively balanced profile with a logarithmic shape. If the erosion capacity is promoted by an increase in rainfall and/or changes of other factors, the profile will become more concave, forming a power shape. The function fitting the longitudinal profile can be used to reflect the stage of erosion evolution of a basin.

2.3.2 Stream power characteristics

The stream power reflects the erosion and sediment transport capacity of a river, and is defined as (Pérez-Peña et al. 2009):

$$\Omega = \gamma Q s \tag{2}$$

where γ is the gravitational constant (9800 N/m³); s is the slope of the water surface, approximately equal to the slope of the riverbed. Q is the water discharge (m³/s). Calculation of Q and s is based on the DEM data and spatially interpolated annual precipitation data of 2007–2016 downloaded from China Meteorological Data Network (http://data.cma.cn/). The elevation of points along the main stream and precipitation and drainage area above each of the points was extracted by hydrological analysis tools of ArcGIS, and the slope was calculated with a 2-km interval of river distance. Water discharge along the main stream was calculated by the following formula on Matlab 2016 software platform:

$$\begin{cases} Q_1 = cA_1 q_1 \\ Q_i = c(A_i - A_{i-1})q_i + Q_{i-1} \end{cases} \tag{3}$$

where Q_1, A_1 and q_1 are the water discharge, drainage area and rainfall of river source, respectively; Q_i and Q_{i-1} are the water discharge, respectively at the points i and i-1; $(A_i - A_{i-1})q_i$ is the water discharge increment between the points i and i-1; q_i is the rainfall at the point i; c is the flow coefficient (Gu et al. 2018).

3 Results

3.1 Neotectonic activity intensity

The calculation of geomorphological indicators shows that the *HI* value is mainly between 0.5–0.6, *AF* value between 67–45, the *SL* value between 183 and 327, and the *Bs* value between 1.77 and 3.62 (Figure 2). Each indicator shows a trend of increasing from north to south, in which the trend of linear increase of *HI* and *SL* values is obvious, while the trend of linear change of *AF* and *Bs* values is not significant. The *IRAT* values of all basins are all greater than or equal to 2, indicating that the regional tectonic activities generally have a moderate-weak intensity. Among them, the TWH and QSH basins have the highest tectonic activity intensity based on the combined results of all the indicators, and their tectonic activities are mainly

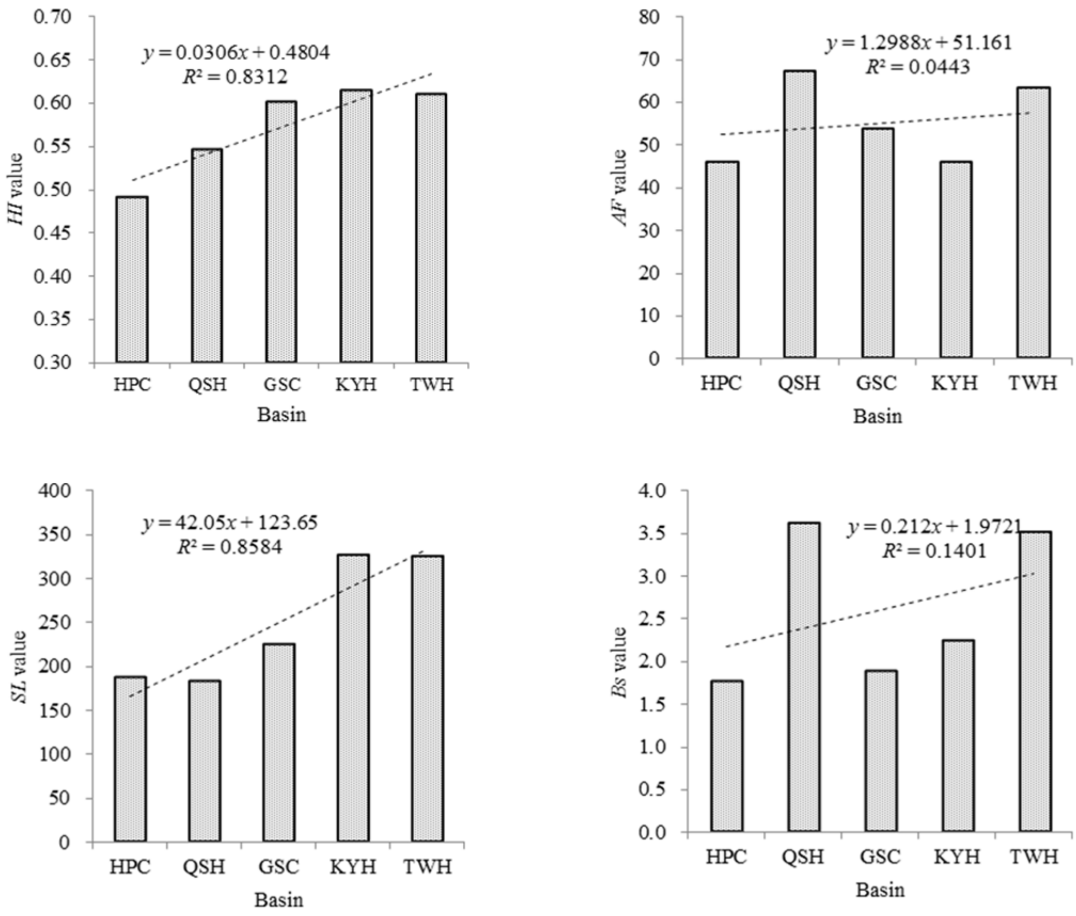

Figure 2 Geomorphological parameters of five basins, including *HI* (hypsometric integral), *AF* (asymmetry factor), *SL* (stream length gradient) and *Bs* (basin shape index), and their spatial trends.

manifested by uplift and left-tilt. In the QSH basin, the *HI* and *SL* values are lower and the *AF* value is larger, and the tilting activity is more prominent. The basins with the weakest tectonic activities are the HPC and GSC (Table 1).

Table 1 Comprehensive evaluation of tectonic activities in the study area

Basins	|*AF*-50| class	*Bs* class	*HI* class	*SL* class	*IRAT* class	Intensity
HPC	3	3	3	3	4	Weak
QSH	1	1	2	3	2	Moderate
GSC	3	3	2	2	4	Weak
KYH	3	2	2	2	3	Weak
TWH	2	1	2	2	2	Moderate

3.2 Erosion characteristics of each basin

The difference between the original surface of the uplifted regional topography built from the high points along the ridges (Figure 3a) and the present surface gives the erosion thickness (Figure 3b). According to the estimates of erosion thickness (Figure 3b and Figure 4a), it is not difficult to find that the most eroded basins are the HPC, KYH and TWH because of the enormous erosion thickness. The areas with the most erosion are mainly located in the middle and upper reaches of HPC, the upper and middle reaches of KYH and the middle reaches of TWH, especially near the main stream. The Pisha sandstone has a median density of 2.45 t/m^3 (Liu et al. 2016), so the historical average of sediment yield modulus is about 182–520 $t/(km^2 \cdot kyr)$, which is 1–284 times less than the modern erosion rate. Area-elevation curves of all basins have great similarities, with a concave shape in the upper reaches and a convex shape in the lower reaches (Figure 4b), indicating that there is a great consistency in erosion pattern in the upper reaches of the basins during the historical period.

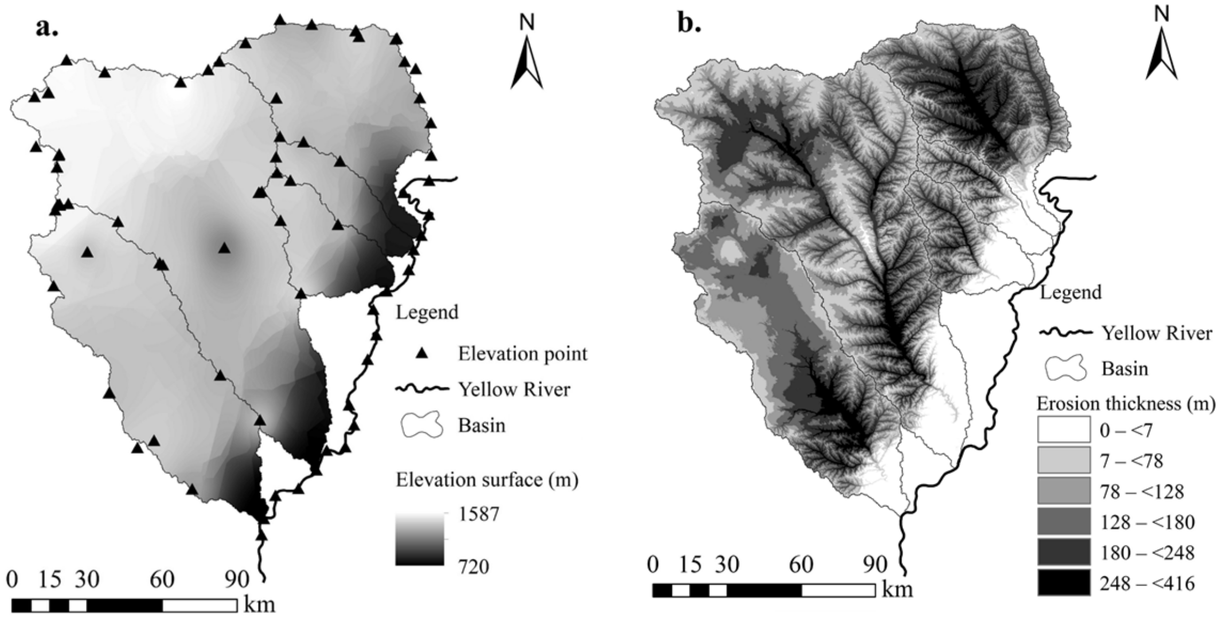

Figure 3 (a) Original surface of the uplifted regional topography and (b) erosion thickness.

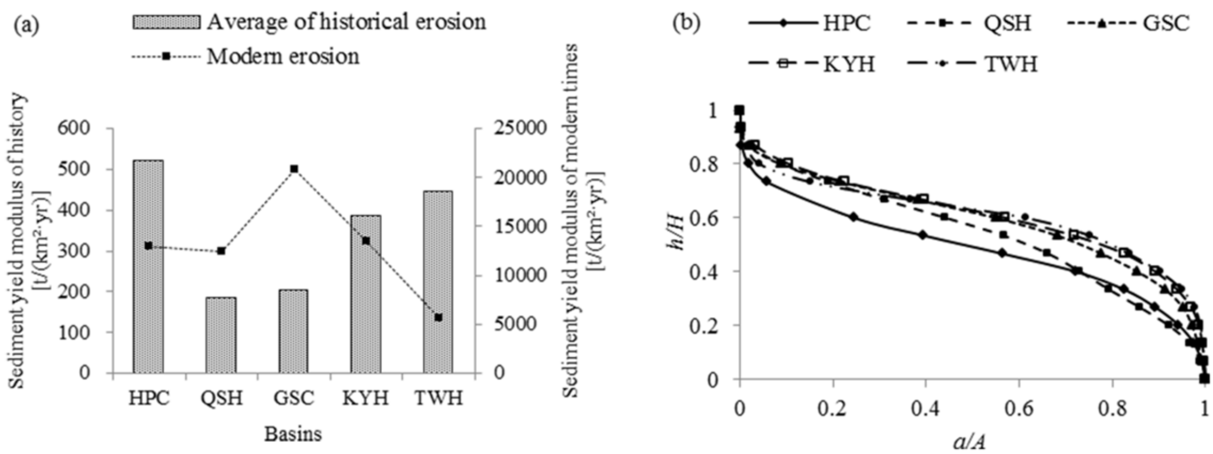

Figure 4 (a) Comparison of historical and modern erosion rates and (b) area-elevation curves. The sediment yield modulus of the HPC, GSC, KYH, and TWH basins are based on measured sediment load and that of the QSH basin comes from the Map of Sediment Yield Modulus in the Loess Plateau of the Yellow River Basin (Zhou 2012).

3.3 Characteristics of longitudinal profile of main stream

The function fitting the longitudinal profile can be used to qualitatively reflect the stage of erosion evolution. The longitudinal profiles of the main streams of the GSC and TWH are linear, and those of the HPC, QSH and KYH are exponential functions (Table 2), so they are all in the early stage of erosion evolution and the erosion potential of each profile is still huge. The *SL*/*K* value reflects the local features of a profile. The steeper the channel is, the higher the *SL*/*K* value is. The higher *SL*/*K* values appear in the middle and lower reaches of each basin (Figure 5). Similarly, the maximum stream power is also distributed in the middle and lower reaches of each basin. The average stream power values are distributed between 4–102 W/m, with the largest in the TWH and the lowest in the QSH (Figure 6 and Figure 7). However, according to the rainfall erosivity factor (*R*) (Sun et al. 2014), rainfall erosion force has an obvious tendency of increasing from north to south, which is consistent with the latitude distribution law of precipitation.

Table 2 Parameters of functions fitting the longitudinal profiles

Profile	Linear function $y=a+bx$			Exponential function $y=ae^{bx}$			Logarithmic function $y=alogx+b$			Power function $y=ax^b$		
	a	*b*	R^2	*a*	*b*	R^2	*a*	*b*	R^2	*a*	*b*	R^2
HPC (Tributary)	1184.5	-3.9×10^{-4}	0.983	1195.1	-4.0×10^{-6}	0.991*	-99.6	2041.5	0.826	2748.5	-0.097	0.797
HPC	1186.0	-3.2×10^{-4}	0.964	1195.2	-6.0×10^{-6}	0.981*	-103.2	2098.6	0.875	2871.3	-0.100	0.847
QSH	1234.1	-4.8×10^{-4}	0.978	1247.2	-5.0×10^{-6}	0.991*	-115.0	2217.5	0.862	3140.4	-0.109	0.824
GSC	1260.3	-5.1×10^{-4}	0.997*	1279.3	-5.0×10^{-6}	0.996	-118.7	2265.1	0.791	3305.3	-0.113	0.748
KYH (Tributary)	1311.8	-2.4×10^{-4}	0.991	1342.7	-2.0×10^{-6}	0.999*	-157.5	2812.6	0.824	5575.4	-0.151	0.771
KYH	1374.0	-2.4×10^{-4}	0.991	1411.4	-2.0×10^{-6}	0.998*	-174.6	3057.3	0.827	6628.8	-0.162	0.768
TWH	1375.4	-3.1×10^{-4}	0.985*	1417.8	-3.0×10^{-6}	0.981	-165.3	2910.1	0.748	5940.3	-0.156	0.693

Note: * the best function type fitting the corresponding profile.

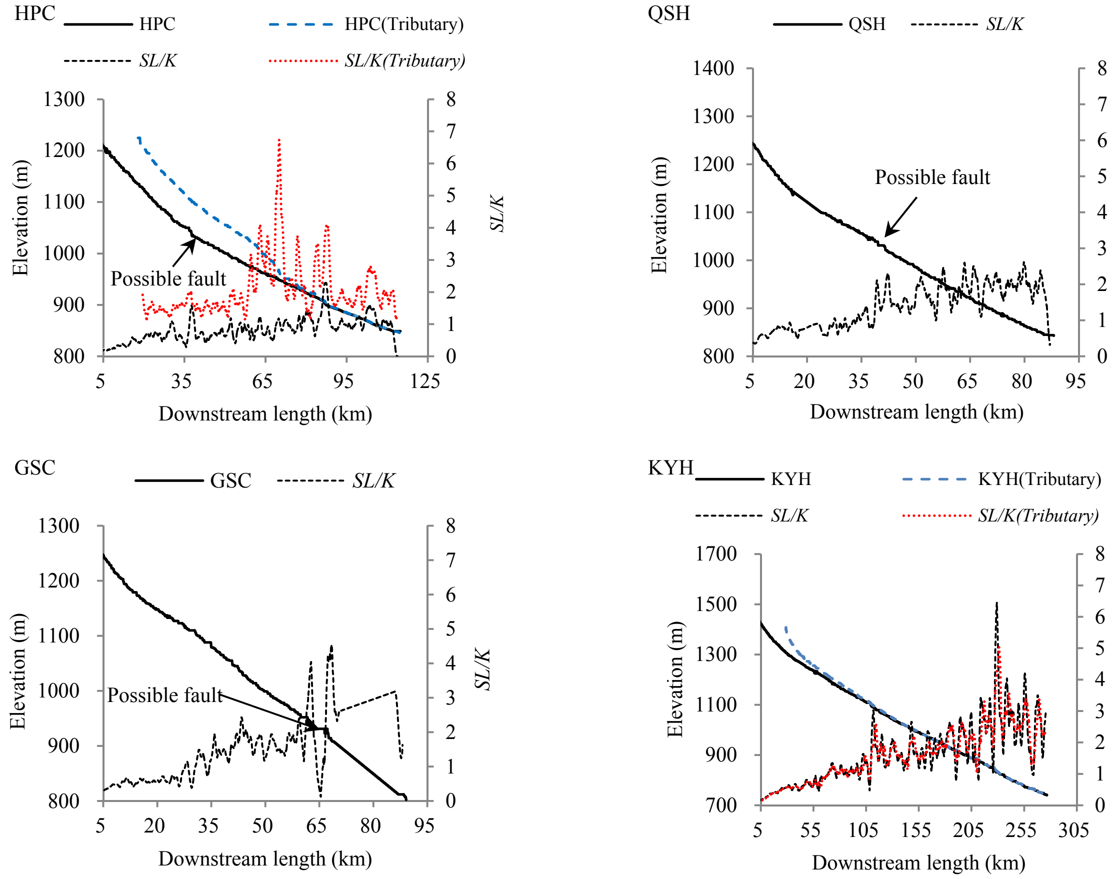

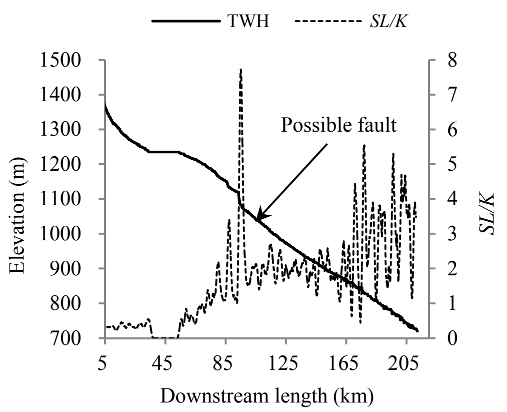

Figure 5 The main longitudinal profiles of five basins and their *SL/K* values. The higher *SL/K* values disclose the locations of segments with a higher slope and a stronger tectonic uplift.

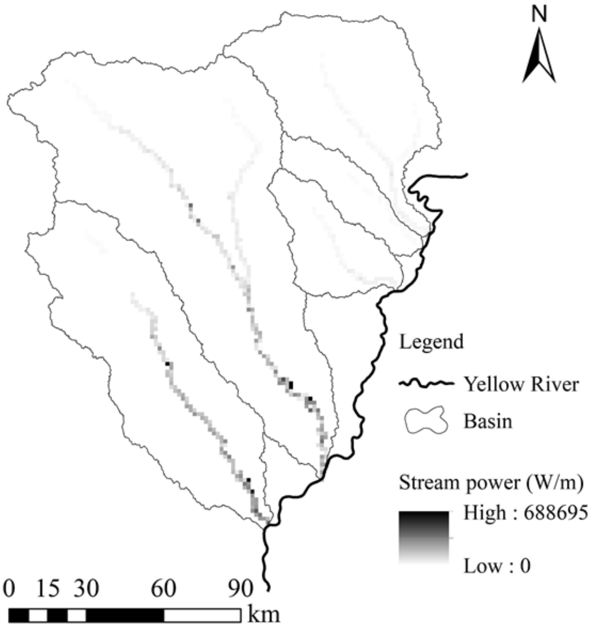

Figure 6 Changes of stream power along main streams.

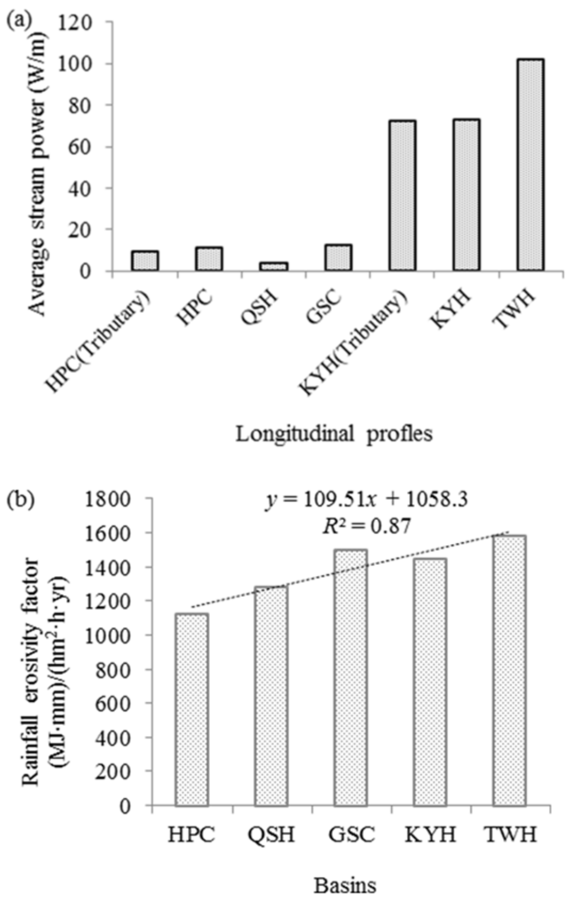

Figure 7 (a) Average stream power and (b) rainfall erosivity factor (based on the rainfall data in 2007-2016).

4 Discussions

Landform evolution of river basins is mainly affected by tectonic activities, hydraulic and lithologic conditions. Among them, tectonic activities and hydraulic conditions are the most direct driving forces for the change of surface morphology. In the study area, since the regional stratigraphy is basically covered by the fluvial and lacustrine sedimentary rocks formed in the Mesozoic, the lithologic differences are not likely to cause large spatial variations in the morphological features of the topography. Therefore, the characteristics of geomorphologic evolution of the study area should be associated principally with the tectonic activity intensity and the characteristics of hydraulic erosion. From the perspective of tectonic activities, the *IRAT* value mainly reflects the general conditions of the basin topography during the uplift and the geomorphic characteristics usually result from the long-term accumulation of the external-internal force actions. According to the characteristics of *AF* values, the watershed showed some degree of tilting during the uplift. The QSH, GSC and TWH basins were tilted to the left, and the tilt in the QSH and TWH watersheds was relatively prominent. Due to the fact that the distribution of *AF* values did not have an obvious spatial variation trend, the formation of this tilting feature was mostly caused by the difference of local uplift rates within each basin. During the process of basin uplift, the increase rate of the longitudinal profile slope of the main stream should generally be higher than that of its branch valleys. As a result, the headward erosion in the main stream caused by the tectonic uplift is always stronger than that in the branch valleys, leading to a lengthening trend in the evolution of the basin and an increase of the *Bs* value (Gao et al. 2013; Ramírez-Herrera 2015). The largest *Bs* in the study area is in the QSH and TWH. With a small drainage area, the QSH has had a limited water discharge, so erosion ability was low and more results of tectonic activities are preserved in the topography of the basin. When the tectonic activity is spatially constant, the variation of the area-elevation curve can reflect the spatial differences of erosion intensity. However, spatial variations in the tectonic activity are common. Thus, the morphological characteristics of the area-elevation curves usually contain the information of both tectonic activity and erosion activity. This means that the convex parts of the curves represent a rapid uplift and a relatively low erosion rate in history, while the concave parts are the opposite. There is a high degree of similarity in the shape of the area-elevation curves of the basins according to the correlation coefficients and their significances (Table 3), but there is also a tendency of change from north to south, reflecting the high degree of consistency and dynamism in the evolution with an insignificant trend. According to the distribution of SL/K values, the steep parts in each longitudinal profile occur in the middle and lower reaches, indicating a large uplift rate there. Similarly, the stream power in these parts is also larger and shows a strong hydraulic cutting ability, but the corresponding area-elevation curve is convex and the downstream longitudinal profile is in a linear form, indicating that the downstream uplift rate is higher. This feature is most prominent in the KYH and TWH, thus it can be further considered that the uplifting rate of the lower reaches of the southern basins is higher than that of the north. Due to the maximum stream power in the lower reaches of each river basin, sediments from the upper reaches are hard to be deposited in the lower reaches but are carried into the Yellow River. Therefore, from the perspective of geomorphic evolution, the current soil and water conservation measures can only work temporarily. The average of sediment yield modulus in geological history is less than the sediment yield modulus of modern times (Figure 4b). The historical average erosion rate was estimated by an erosion onset time of 1.41 Ma BP. Actually, according to some scholars' findings, the Ordos block has completed its conversion from a basin to a plateau before 1.41 Ma BP (Yue et al. 2007), suggesting that erosion started before 1.41 Ma BP and the historical average erosion rate should be less than the estimate of this article. This is partly because the tectonic uplift of the Quaternary has been continuously strengthened and the terrain conditions have become favorable for erosion. On the other hand, due to climate warming during the Holocene, rainfall may have increased and the hydro-erosion activities may have become relatively active. In recent decades, although some soil and water conservation measures have been taken, the erosion intensity is still far greater than the historical average level, and except for the HPC basin, it follows the trend of increasing from north to south (Figure 4a), which can be attributed to the changes in the precipitation erosion force and the distribution of stream power (Figure 6 and Figure 7). It is found that the erosion rate of the study area is higher than that of the whole Loess Plateau and lower than that of the gully region of the Loess Plateau (Table 4). This characteristic may be related to the corrosion resistance of Pisha sandstone being greater than that of loess.

Table 3 Correlation coefficients of area-elevation curves. HPC, QSH, GSC, KYH, and TWH are the five basins

	HPC	QSH	GSC	KYH	TWH
HPC	1	0.9805*	0.9586*	0.9509*	0.9489*
QSH		1	0.9924*	0.9881*	0.9848*
GSC			1	0.9994*	0.9979*
KYH				1	0.9986*
TWH					1

Note:*Significant at α = 0.05.

5 Conclusions

Based on the comparison of geomorphic indexes, this paper analyzed the historical erosion, the stream power, and the dynamic characteristics of geomorphologic evolution in several basins in the eastern wing of Ordos Plateau. The results show that the intensity of tectonic activities in the

Table 4 Comparison of erosion rates in the five basins and different areas of Loess Plateau

Age (ka BP)	Erosion rate in five basins t/(km²·yr)					Entire Loess Plateau (Li and Lu 2010)		Loess Plateau hilly-gully region (Ma et al. 1993)	
	HPC	QSH	GSC	KYH	TWH	Age (ka BP)	Erosion rate t/(km²·yr)	Age (ka BP)	Erosion rate t/(km²·yr)
Modern	12982	57	20835	13439	5614	0–12	93.02	6	16834.61
1410–Modern	520	182	203	384	443	12–74	47.35	25	11050.19
						74–130	41.60	115	3341.87
						130–190	74.27		
						190–250	44.76	225	3046.43

basins was generally moderate-weak, with an unconspicuous increasing trend from north to south. The form of tectonic activity of the basins was mainly uplifting, and some basins tilted at a certain extent. The uplift rates in the lower reaches of each basin were greater than the erosion rates, especially in the KYH and TWH basins. During the uplift of the regional topography, the most serious erosion was generally concentrated in the upper and middle reaches of the main stream. At present, the longitudinal profiles of the main streams have an exponential and nearly linear form, which suggest that they are in the early stage of erosion evolution. The mechanisms of geomorphologic evolution in different basins have a great similarity, but there is also a tendency of changing from north to south. The conservative estimate of historical average erosion rate should be less than 182–520 t/(km^2·yr), much less than that of the modern times. The mean stream power is between 4 and 102 W/m, with the largest in the KYH and TWH and the lowest in the QSH. The maximum stream power generally appears in the downstream reaches, which is the main reason for direct injection of sediments into the Yellow River. From the perspective of geomorphological evolution, the current soil and water conservation measures can hardly cure the erosion and sediment yield of these basins in the long term.

Acknowledgements

This work was supported by the National Natural Science Foundation of China (Grant No. 41671004). We are very grateful to the three anonymous reviewers and the editors for their detailed and valuable suggestions.

References

Cheng S, Deng Q, Zhou S, et al. (2002) Strath terraces of Jinshaan Canyon, Yellow River, and Quaternary tectonic movements of the Ordos Plateau, North China. Terra Nova 14(4): 215-224. https://doi.org/10.1046/j.1365-3121.2002.00350.x

Deng Q, Cheng S, Min W, et al. (1999) Discussion on Cenozoic tectonics and dynamics of Ordos block. Journal of Geomechanics 5(3): 13-21. (In Chinese)

Gao L, Hou D, Li J, et al. (2016a) Movement characteristics and present seismic activity of Ordos Block. Geodesy and Geodynamics 7(6): 451-458. https://doi.org/10.1016/j.geog.2016.07.008

Gao M, Zeilinger G, Xu X, et al. (2016b) Active tectonics evaluation from geomorphic indices for the central and the southern Longmenshan range on the Eastern Tibetan Plateau, China. Tectonics 35(8): 1812-1826. https://doi.org/10.1002/2015TC004080

Gao M, Zeilinger G, Xu X, et al. (2013) DEM and GIS analysis of geomorphic indices for evaluating recent uplift of the northeastern margin of the Tibetan Plateau, China. Geomorphology 190(439): 61-72. https://doi.org/10.1016/j.geomorph.2013.02.008

Gu Z, Shi C, Yang H (2018) Responses of riverbed particles to geomorphologic processes in aeolian-fluvial action area: A case of the Heilaigou basin in Inner Mongolia of China. Journal of Resources and Ecology 9(2): 191-201. https://doi.org/10.5814/j.issn.1674-764x.2018.02.009

Hack JT (1973) Stream profile analysis and stream gradient index. Journal of Research of the U.S. Geological Survey 1(4): 421-429. https://pubs.er.usgs.gov/publication/70161653

Hamdouni RE, Irigaray C, Fernández T, et al. (2008) Assessment of relative active tectonics, southwest border of the Sierra Nevada (southern Spain). Geomorphology 96(1): 150-173. https://doi.org/10.1016/j.geomorph.2007.08.004

Hu Z, Pan B, Guo L, et al. (2016) Rapid fluvial incision and headward erosion by the Yellow River along the Jinshaan gorge during the past 1.2 Ma as a result of tectonic extension. Quaternary Science Reviews 133: 1-14. https://doi.org/10.1016/j.quascirev.2015.12.003

Ji Y, Gao H, Pan B, et al. (2011) Implication of active structure in the upper reaches of Weihe River basin from stream length-gradient index (SL index) and Hack profile. Journal of Lanzhou University (Natural Science) 47(4): 1-47. (In Chinese)

Li L, Lu H (2010) A preliminarily quantitative estimation of the sedimentation and erosion rates of loess deposits in Chinese Loess Plateau over the past 250 ka. Acta Geographica Sinica 65(1): 37-52. (In Chinese)

Liu H, Shi M, Cai H, et al. (2016) Experimental study of the physical characteristics of the Pisha sandstone on its erosion. Yellow River 38(6): 8-10. (In Chinese)

Liu L, Liu XH (2010) Sensitivity analysis of soil erosion in the northern Loess Plateau. Procedia Environmental Sciences 2(1): 134-148. https://doi.org/10.1016/j.proenv.2010.10.017

Ma L (2007). China's Geological Atlas. Beijing, Geological Publishing House. (In Chinese)

Ma XZ, , Lu ZC, Jin DS (1993) Evolution and dissipative structure in the drainage-geomorphic system. Acta Geographica Sinica 48(4): 367-375. (In Chinese)

Mahmood SA, Gloaguen R (2012) Appraisal of active tectonics in Hindu Kush: Insights from DEM derived geomorphic indices and drainage analysis. Geoscience Frontiers 3(4): 407-428. https://doi.org/10.1016/j.gsf.2011.12.002

Owono FM, Ntamak-Nida MJ, Dauteuil O, et al. (2016) Morphology and long-term landscape evolution of the South African plateau in South Namibia. Catena 142: 47-65. https://doi.org/10.1016/j.catena.2016.02.012

Pan B, Hu Z, Wang J, et al. (2011) A magnetostratigraphic record of landscape development in the eastern Ordos Plateau, China: Transition from Late Miocene and Early Pliocene stacked sedimentation to Late Pliocene and Quaternary uplift and incision by the Yellow River. Geomorphology 125(1): 225-238. https://doi.org/10.1016/j.geomorph.2010.09.019

Pike RJ, Wilson SE (1971) Elevation-relief ratio, hypsometric integral, and geomorphic area-altitude analysis. Geological Society of America Bulletin 82(4): 1079-1083. https://doi.org/10.1130/0016-7606(1971)82[1079:ERHIAG]2.0.CO; 2

Rădoane M, Rădoane N, Dan D (2003) Geomorphological

evolution of longitudinal river profiles in the Carpathians. Geomorphology 50(4): 293-306. https://doi.org/10.1016/S0169-555X(02)00194-0
Ramírez–Herrera MT (2015) Geomorphic assessment of active tectonics in the Acambay graben, Mexican Volcanic Belt. Earth Surface Processes & Landforms 23(4): 317-332. https://doi.org/10.1002/(SICI)1096-9837(199804)23:4<317::AID-ESP845>3.0.CO;2-V
Ran D, Luo Q, Zhou Z, et al. (2008) Sediment retention by check dams in the Hekouzhen-Longmen Section of the Yellow River. International Journal of Sediment Research 23(2): 159-166. https://doi.org/10.1016/S1001-6279(08)60015-3
Shi W (2008) DEM drainage analysis of the Shanxi-Shaanxi gorge in the middle reaches of the Huanghe River and its neotectonic implications. Quaternary Research 28(2): 288-298. (In Chinese)
Pérez-Peña JV, Azañón JM, Azor A, et al. (2009) Spatial analysis of stream power using GIS: SLK anomaly maps. Earth Surface Processes and Landforms 34: 16-25. https://doi.org/10.1002/esp.1684
Sun W, Shao Q, Liu J, et al. (2014) Assessing the effects of land use and topography on soil erosion on the Loess Plateau in China. Catena 121: 151-163. https://doi.org/10.1016/j.catena.2014.05.009
Yue LP, Li JX, Zheng GZ, et al. (2007) Evolution of the Ordos Plateau and environmental effects. Science in China (Series D: Earth Sciences) 50(2): 19-26. https://doi.org/10.1007/s11430-007-6013-2
Zhang K, Li S, Peng W, et al. (2004) Erodibility of agricultural soils on the Loess Plateau of China. Soil & Tillage Research 76(2): 157-165. https://doi.org/10.1016/j.still.2003.09.007
Zhou YL (2012) Atlas of Soil and Water Conservation in the Yellow River Basin. Beijing, Seismological Press. (In Chinese)
Zuo D, Xu Z, Yao W, et al. (2016) Assessing the effects of changes in land use and climate on runoff and sediment yields from a watershed in the Loess Plateau of China. Science of the Total Environment 544: 238-250. https://doi.org/10.1016/j.scitotenv.2015.11.060